# Probing the Photonic Properties of a Cholesteric Elastomer under Biaxial Stress

**Jürgen Schmidtke***

*Physikalisches Institut, Albert-Ludwigs-Universität, Hermann-Herder-Strasse 3, D-79104 Freiburg, Germany*

**Simon Kniesel and Heino Finkelmann**

*Institut für Makromolekulare Chemie, Albert-Ludwigs-Universität, Stefan-Meier-Strasse 31, D-79104 Freiburg, Germany*

*Received June 22, 2004; Revised Manuscript Received December 3, 2004*

ABSTRACT: We have investigated the photonic properties of a free-standing cholesteric elastomer film under biaxial mechanical load. The sample, which was obtained by UV cross-linking of a cholesteric side-chain polymer, shows substantially improved optical properties compared to cholesteric elastomers obtained by the anisotropic deswelling method. The selective reflection of circularly polarized light and the modified spontaneous emission of dispersed fluorescent guest molecules show that the cholesteric order is well preserved in the cross-linked film. Application of biaxial stress leads to a shift of the photonic stop band to shorter wavelengths due to a contraction of the cholesteric helix; the change of the cholesteric pitch is affine to the film thickness. Pulsed excitation of the fluorescent guest molecules gives rise to photonic band edge laser emission, which is mechanically tunable in a wavelength range of almost 100 nm. The lasing performance is found to be comparable to that of conventional cholesteric systems.

## 1. Introduction

Cholesteric liquid crystals (CLCs) are formed by rodlike molecules (the so-called mesogens), which arrange themselves in a periodic helical order.[1] The resulting twisted birefringent medium acts as a polarization-sensitive one-dimensional photonic crystal: propagation of circularly polarized light with the same handedness as the cholesteric helix is forbidden in a certain frequency range[2]. The photonic stop band is centered at $\lambda_R = \bar{n}p$ and has a width $\Delta\lambda = \Delta np$, where $p$ is the pitch of the cholesteric helix, $\bar{n} = (n_o + n_e)^{1/2}/2$ is the average refractive index of the nematic planes, and $\Delta n = n_e - n_o$ is their birefringence. The photonic band structure gives rise to the well-known selective reflection of circularly polarized light and to modified spontaneous emission of fluorescent guest molecules.[3−6] Moreover, due to the presence of resonant optical modes at the photonic band edges, dye-doped CLC films can act as mirrorless lasers.[4,7−11]

Liquid crystalline elastomers[12] are unique materials combining rubber elasticity and liquid crystalline phase structure. The elastic coupling of liquid crystalline order and polymer network results in anisotropic elastic properties and allows for controlled distortions of the liquid crystalline phase structure by applying mechanical stress. In the case of cholesteric elastomers, mechanical stress affects the helicoidal ordering of the mesogenic moieties and therefore changes the photonic band structure. Transmission measurements[10] have shown that a biaxial strain perpendicular to the cholesteric helix results in a shortening of the cholesteric pitch, affine to the sample dimension along the cholesteric helix. It has been predicted[13] that a uniaxial strain perpendicular to the cholesteric helix should lead to a distortion, and for large strains finally to an unwinding, of the cholesteric helix. Band structure calculations[14] predict the appearance of additional band gaps, some of them 'total' (i.e., polarization-independent). Experimental evidence for a distorted cholesteric helix in uniaxially stretched CLC elastomer films has been obtained by Cicuta et al.[15] by wide-angle X-ray diffraction.

In the first attempts to obtain CLC elastomer films with uniform planar cholesteric order, the so-called anisotropic deswelling method[16] was employed: during the network formation, a uniaxial deswelling process is initiated, resulting in an overall orientation of the cholesteric helix along the film normal. However, the optical properties of such films are far from perfect. The selective reflection band is blurred, and the lasing threshold of dye-doped samples is 3 orders of magnitude higher than that of conventional CLC films.[10] We followed an alternative synthetic approach to obtain CLC elastomer films with improved optical properties, similar to a well-established procedure to obtain thin smectic monodomain elastomer films:[17] first, between two glass substrates, a uniformly oriented film is formed by an un-cross-linked CLC polymer. After photo-cross-linking of the film and removal of the substrates, we obtain thin free-standing CLC elastomer films with Grandjean texture (uniform orientation of the cholesteric helix parallel to the film normal).

In this paper, we present an optical characterization of the these new cholesteric elastomers. In addition to transmission measurements, we probed the photonic band structure of the elastomer by fluorescent guest molecules. On application of biaxial strain, we find a continuous shift of the stop band to shorter wavelengths, which allows for a tuning of the photonic band edge laser emission over a range of almost 100 nm.

## 2. Experimental Section

**2.1. Film Preparation.** Cholesteric elastomers of 20 $\mu$m thickness were synthesized according to a procedure which will

* Author to whom correspondence should be addressed. E-mail: juergen.schmidtke@physik.uni-freiburg.de.

10.1021/ma0487655 CCC: $30.25 
Published on Web 01/19/2005

be described in detail elsewhere. A photo-cross-linkable polymer was synthesized via polymer analogous hydrosilylation of poly[oxy(methylsilylene)]. To a solution of 2.494 mmol of **1** ($DP_n = 260$), 0.3167 mmol of **2**, 1.6236 mmol of **3**, 0.379 mmol of **4**, and 0.175 mmol of **5** in 1.5 mL of toluene 20 $\mu$L of a

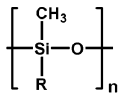


(1)

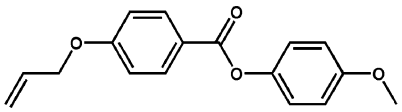

(2)

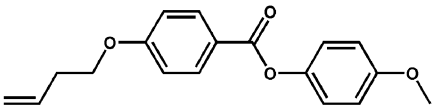

(3)

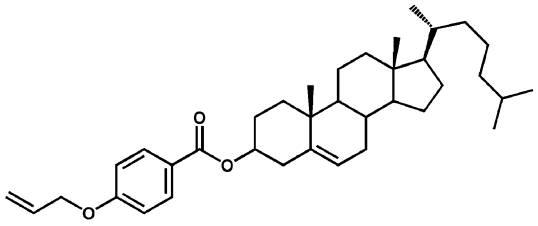

(4)

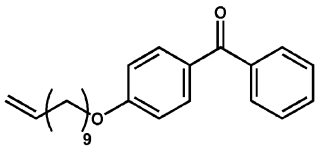


(5)

1 wt% solution of the Pt catalyst SLM86005 (Wacker Chemie, Burghausen) in $CH_2Cl_2$ ($6 \times 10^{-4}$ mmol) was added. This solution was stirred at 60 °C in darkness. After a further 5 and 14 h, 20 $\mu$L of the catalyst solution was added. The progress of the reaction was monitored using IR spectroscopy ($\nu_{Si-H} = 2160$ cm$^{-1}$). The resulting polymer was purified via reprecipitation (five times) from methanol. Dry-freezing yielded the photo-cross-linkable polymer (~80%). To achieve lasing, the purified polymer was doped with 0.2 wt% of the laser dye DCM, which has the following structure.

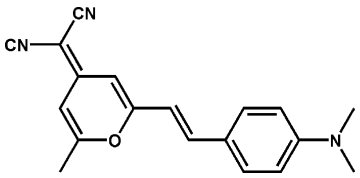


The dye-doped polymer was prepared between two glass substrates covered with a water soluble sacrificial layer (PEOX (poly(2-ethyl-2-oxazoline)). To obtain elastomers with a well-defined thickness (20 $\mu$m), the cavity between the two glass plates was formed by spacer foil strips which were placed between the glass plates. The sample was then annealed within the liquid crystalline state for 2 days in order to achieve a Grandjean texture. The annealing temperature was adjusted 10 K below the clearing temperature of the liquid crystalline polymer ($T_{ni} = 104 \pm 1$ °C) for 2 days. Due to interface interactions, well-oriented samples were obtained. The orientation process of the liquid crystalline polymers was monitored using visible absorption spectroscopy and polarization microscopy. The oriented film was cross-linked when the line shape of the selective reflection band did not change any more. The cross-linking process is based on the radical reaction of the benzophenone derivative[18] (**5**) which is attached to the polymer backbone. To perform the cross-linking, the sample was

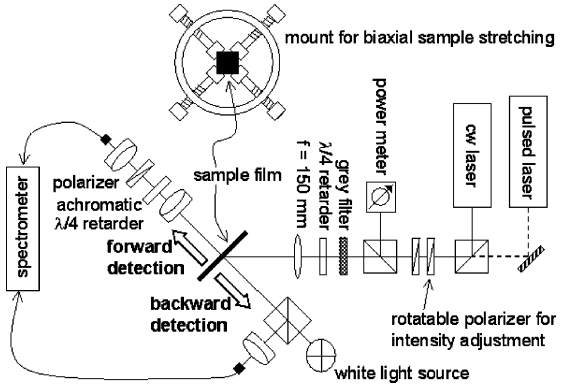


**Figure 1.** Sketch of the experimental setup.

irradiated with pulsed UV light of a 'Dentacolor XS' lamp (Kulzer, Germany) for three minutes from both sides. After the cross-linking reaction was completed, the resulting elastomer film was removed from the glass substrate by dissolving the sacrificial layer in water. After 2 days, the sacrificial layer was dissolved and the free-standing elastomer film was available. It is possible to improve the optical properties of cholesteric polymers and elastomers (selective reflection, optical transparency) by attaching of mesogenic side groups with different numbers of carbon atoms in the spacer unit between the polymer chain of the mesogenic side groups. Therefore, prior to performing the laser experiments, the polymers were synthesized using a mixture of mesogens with 3 and 4 carbon atoms in the spacer unit (**2**−**4**).

**2.2. Optical Setup.** Experiments were performed with the setup shown in Figure 1, which allows for successive transmission, fluorescence, and lasing experiments at the same sample spot. We used three light sources to probe the sample: a well collimated white light source (beam diameter in the sample plane ≈ 1.5 mm) for transmission measurements, a cw second harmonic Nd:YAG laser (Coherent 532−200, $\lambda = 532$ nm) as excitation source for fluorescence measurements, and the frequency-doubled pulses of a *Q*-switched Nd:YAG laser (Quanta Ray DCR2, pulse duration ≈ 7 ns) as pump source to excite laser emission (spot diameter of the focused beam ≈ 20 $\mu$m). To minimize back reflection by the film, we used r-cp excitation beams for the fluorescence and lasing experiments (as the sample has a left-handed cholesteric helix, an r-cp beam essentially resembles the normal mode which is unaffected by the cholesteric medium). We simultaneously detected the 'forward' and 'backward' emitted light (as indicated in Figure 1), using two separate spectrometers (Ocean Optics S2000, resolution $\Delta\lambda = 1.5$ nm). The forward emission of the film, as well as the transmitted white light, was decomposed in left- and right-handed circularly polarized contributions by an 'superachromatic' quarter-wavelength retarder (B. Halle Nachfl. GmbH, Berlin) and a rotatable analyzer. To perform measurements on a free-standing sample, a square sheet of the elastomer film (size = 1 cm$^2$) was fixed at its four corners on a mount as sketched in Figure 1, which allows for a controlled stretching of the sample. One should note that a symmetrically applied strain of the film at its corners of course does not result in an overall biaxial deformation of the sample; near the edges there are substantial shear contributions, and near the corners the deformation is dominated by a uniaxial strain. However, an almost perfect biaxial strain is to be expected in the central region of the film.

**2.3. Refractive Index Measurements.** Measurements were performed with an Abbe refractometer at room temperature. The ordinary and extraordinary refractive indices, $n_{o,CLC}$ and $n_{e,CLC}$, of the CLC elastomer films are related to the refractive indices, $n_o$ and $n_e$, of a respective untwisted (nematic) birefringent medium via $n_o = n_{e,CLC}$ and $n_e^2 = (2n_{o,CLC}^2 - n_{e,CLC}^2)^{1/2}$.

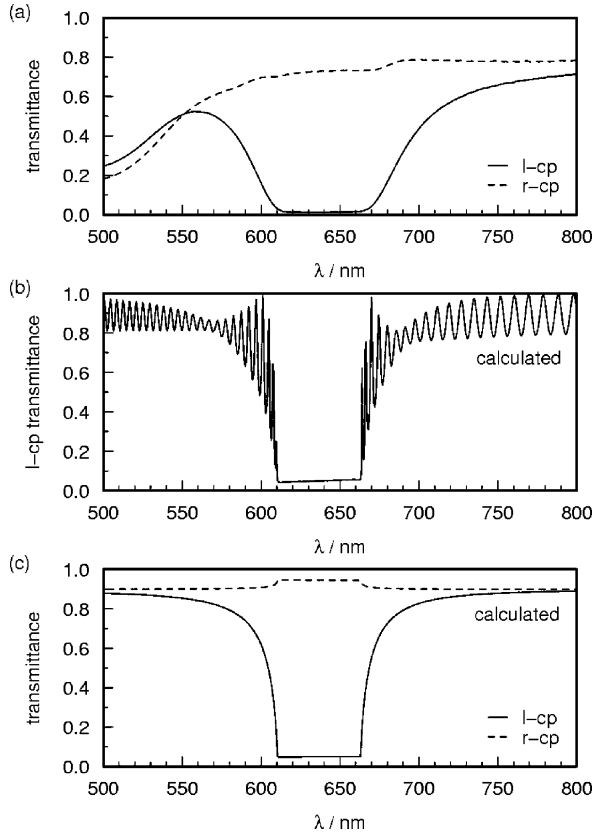


**Figure 2.** Undeformed elastomer film: l-cp and r-cp transmittance curves (a). Simulated l-cp transmittance curve for an ideal CLC monodomain film (b). Theoretical l-cp and r-cp transmittance curves, neglecting multiple reflections (c). In (b) and (c), absorption of the film is neglected.

## 3. Results

**3.1. Undeformed Film.** In Figure 2a, the left- and right-handed ('l-cp' and 'r-cp') transmittances of the relaxed CLC elastomer film are shown. The l-cp transmission curve shows a very pronounced selective reflection band (centered at 637.3 nm), whereas the r-cp transmission is hardly affected by the cholesteric order. The drop in transmission at short wavelengths is due to absorption of the dispersed dye.

We simulated the l-cp transmission of an ideal CLC monodomain with the same optical and structural parameters (handedness, cholesteric pitch, refractive indices, and film thickness) as the sample under investigation, using the fast version[19] of the numerical Berreman method.[20] We find good qualitative agreement between the experimental result and the simulated transmission curve (Figure 2b). The simulated curve shows Fabry−Perot interference fringes due to multiple reflection at the CLC−air interface. In the experimental curve, they are absent. It is well known from low-molar-mass CLC films that small spatial variations in the structural parameters of the cholesteric order are sufficient to smear out the pattern of the interference fringes. In addition, they may also be suppressed by a certain amount of surface roughness of the elastomer film. To account for this, we have additionally computed l-cp and r-cp transmission curves, neglecting multiple reflection (Figure 2c). The trenchlike l-cp transmission profile qualitatively matches the experimental result. However, the waist of the trench (full-width-half-minimum) of the measured curve is roughly 1.5 times as wide as the theoretical one (measured ≈ 107 nm; theoretical ≈ 63 nm). Obviously, no pure cholesteric order is present in the sample. A possible reason for the broadening of the selective reflection band is a slight variation of the cholesteric pitch along the film normal: in a simple coarse-grained picture, such a system may be considered as a stack of cholesteric sublayers with varying helical pitches and, accordingly, with varying locations of the selective reflection band. The individual selective reflection bands of the sublayers then add up to a broadened selective reflection band of the complete system. Indeed, by introduction of a pitch gradient along the helical axis, broad-band circularly polarized reflectors can be realized.[21] The photonic stop band also slightly affects the r-cp transmission. However, while it shows up in the theoretical curve as a somewhat elevated plateau, in the experimental curve, there is a slightly reduced r-cp transmission in the region of the stop band. One should also note that, for all wavelengths, the l-cp, as well as the r-cp transmission, of our sample is significantly smaller than theoretically predicted for an ideal CLC film. This holds not only in the region of dye's absorption band (where this is to be expected, as absorption is neglected in the calculated curves of Figure 2) but also at large wavelengths, far away from the reflection band, e.g., for $\lambda = 800$ nm, experimental l-cp and r-cp transmittances are 0.714 and 0.782, while the respective computed values are 0.890 and 0.899. As the liquid crystalline polymer used for the sample film is almost nonabsorbing for visible light, the reduced overall transmission is obviously due to scattering losses. Possible reasons for this are rough film surfaces or internal heterogeneities of the film. The transmission properties are essentially the same as those of the CLC polymer film before crosslinking; however, the cholesteric order might also be slightly affected by small strains which are unavoidable to smooth out the free-standing sample film on the mount.

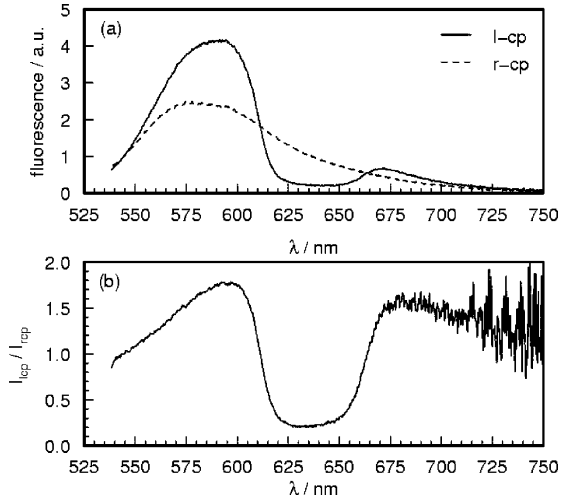


**Figure 3.** Undeformed elastomer film: fluorescence, decomposed in l-cp and r-cp emission contributions (a), and the ratio $I_{lcp}/I_{rcp}$ of the circularly polarized emission contributions (b).

The photonic stop band strongly affects spontaneous emission of the dispersed fluorescent dye (Figure 3a): the r-cp contribution is quite flat and essentially resembles the emission spectrum of the dye in an ordinary, isotropic solvent. The l-cp contribution, however, is strongly reduced inside the stop band, and it is enhanced near the band edges. In earlier work,[6] we have studied the emission properties of well-oriented low-

molar-mass CLC films. They show a sharp drop of the l-cp contribution almost to zero intensity and sequences of emission peaks framing the photonic stop band. In the case of the elastomer, the effect of the stop band on the emission is less pronounced: the dip in the l-cp emission spectrum is quite smooth, and no sharp band edge emission peaks are observed. The ratio $I_{lcp}/I_{rcp}$ of the circularly polarized emission contributions is shown in Figure 3b. The relative l-cp emission enhancement is almost symmetrical at both band edges. This is in contrast to conventional CLC films doped with DCM, where so far, a dominant enhancement at the long wavelength band edge has always been observed. Such an asymmetry of emission enhancement indicates an anisotropic orientational distribution of the dye's transition dipole moment with respect to the local director, which is due to the partial alignment of the dye molecules in their locally nematic environment.[6] Regarding the almost symmetric intensity enhancement we find for our elastomer, one might be tempted to deduce an isotropic orientational distribution of the dispersed dye molecules. However, this seems very unlikely: in conventional CLC films, the nematic order parameter of the transition dipole moment of the excited DCM molecules has been found to be definitely positive (order parameters as large as 0.4 were obtained[6]). Although there are still slight discrepancies in the optics of the elastomer and of an ideal CLC, the transmission and fluorescence measurements clearly indicate a substantial improvement in the cholesteric order compared to CLC elastomers obtained by the anisotropic deswelling method.

**3.2. Film under Biaxial Load.** On application of biaxial stress, the selective reflection band shifts to shorter wavelengths, while the r-cp transmission is hardly affected (Figure 4). In Figure 5, the l-cp transmission curves are plotted together as a function of the reduced wavelength $\lambda/\lambda_R$. The shape of the selective reflection band, and in particular the relative width wavelength $\Delta\lambda/\lambda_R$, does not substantially change under biaxial strain (the deviations in the region of the short-wavelength band edge can be fully ascribed to the increasing overlap of the photonic stop band and the absorption band of the fluorescent dye). Obviously, the cholesteric order is well preserved in the strained film. From the change in absorption of the dispersed dye, the relative change of the film thickness at the examined sample spot can be determined. In Figure 6 the relation between stop band wavelength, $\lambda_R$, and relative film thickness $d/d_0$ is shown ($d_0$ is the thickness of the relaxed film, and $d$ is the thickness of the deformed film at the examined spot). We find, within experimental error, a linear relation which can be extrapolated to zero $\lambda_R$ for vanishing film thickness: the change of the cholesteric pitch, which determines the stop band wavelength, $\lambda_R$, therefore is affine to the film thickness.

The continuous shift of the photonic stop band on increasing biaxial strain also shows up in the fluorescence spectra (Figure 7). The emission enhancement at the short-wavelength band edge vanishes for large deformations due to the increasing overlap of the stop band and the dye's absorption band (the long dwell times of emitted photons inside the film then strongly support reabsorption). The ratio $I_{lcp}/I_{rcp}$ of the circularly polarized emission contributions, obtained for various applied biaxial strains, is shown in Figure 8 as a function of the reduced wavelength $\lambda/\lambda_R$. Except for the strain-dependent reabsorption at short wavelengths mentioned above, the overall shape of the curves remains essentially the same for all applied strains. This is a further confirmation that the helical order is hardly affected by the biaxial strain.

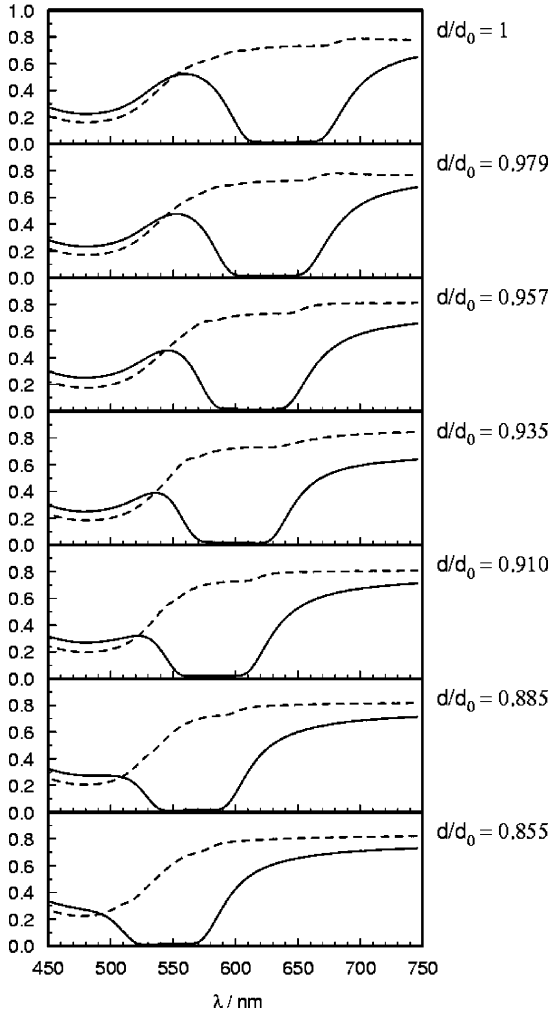


**Figure 4.** Evolution of the l-cp (solid curves) and r-cp (dashed curves) transmittance of the CLC elastomer film on increasing biaxial strain (as indicated on the right of each graph). The transmission curves were obtained for illumination of the film center, where the sample undergoes an almost homogeneous biaxial deformation.

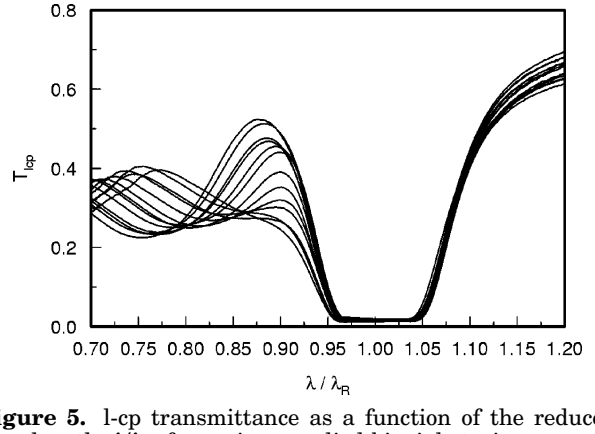


**Figure 5.** l-cp transmittance as a function of the reduced wavelength, $\lambda/\lambda_R$, for various applied biaxial strains.

**3.3. Laser Emission.** Using pulsed excitation, we observe laser emission at the long-wavelength band edge. On application of a biaxial strain, the laser line

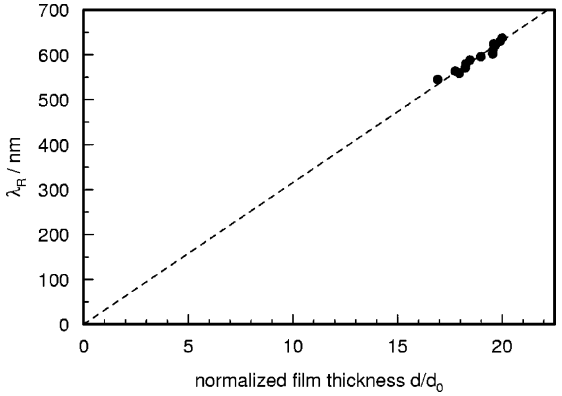


**Figure 6.** Stop band center, $\lambda_R$, as a function of the relative film thickness, $d/d_0$.

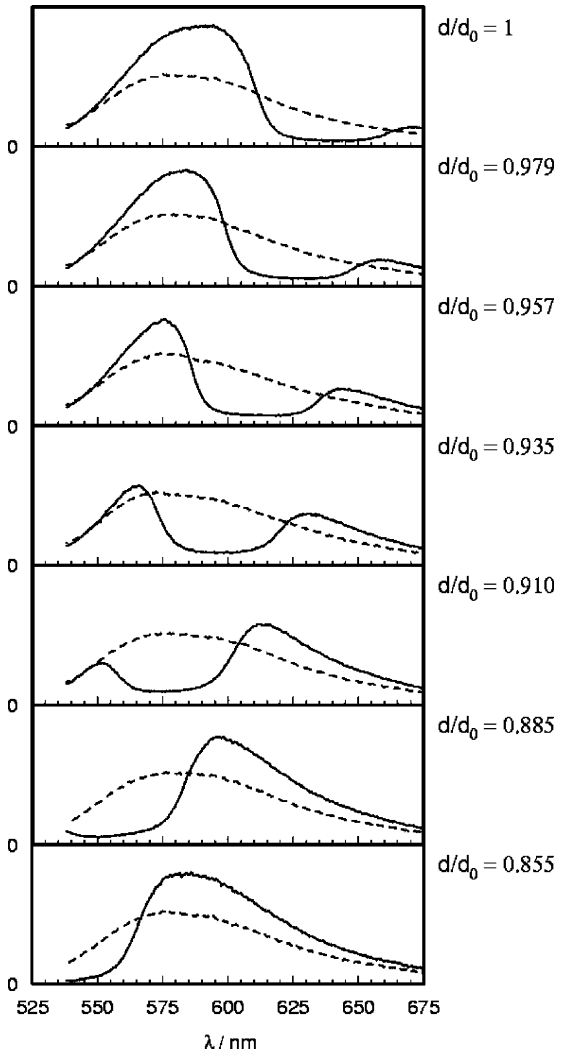


**Figure 7.** Evolution of the l-cp (solid curves) and r-cp (dashed curves) fluorescence contributions of the CLC elastomer film on increasing biaxial strain (as indicated on the right of each graph).

is tuned toward shorter wavelengths due to the shift of the photonic band gap (Figure 9). For the unstrained sample, lasing performance is poor: the stop band is far away from the dye's emission maximum, and therefore, the film provides little optical gain at the photonic band edge resonances. On increasing strain, the overlap of the stop band and the dye's emission maximum improves, and therefore, laser emission increases. For the highest applied strains, the lasing efficiency drops

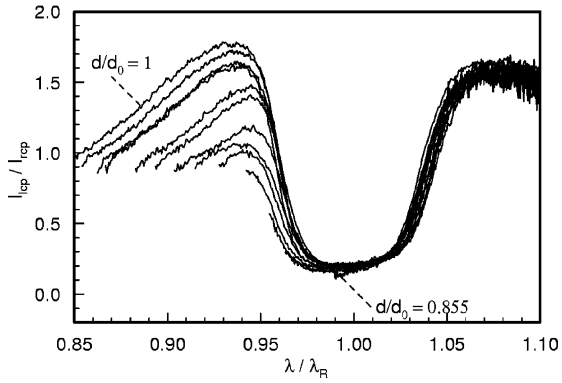


**Figure 8.** Ratio, $I_{lcp}/I_{rcp}$, of the circularly polarized emission contributions. Curves are plotted for various biaxial strains as a function of the reduced wavelength, $\lambda/\lambda_R$.

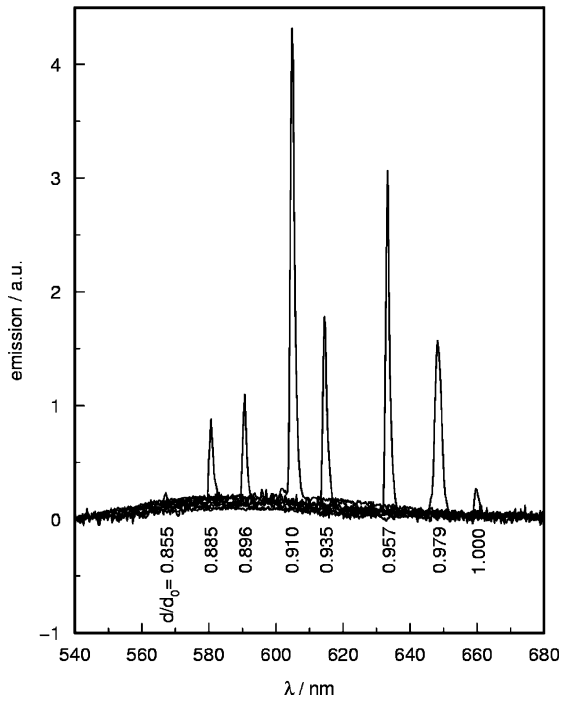


**Figure 9.** Laser lines observed for various applied biaxial deformations.

down again due to the decreasing gain and increasing overlap with the dye's absorption band at the resonance wavelength.

Laser emission of well-ordered low-molar-mass CLCs is found to be highly directional (see, e.g., ref 22), resulting in clear-cut laser spots. For the CLC elastomer, the intensity profile of the laser spot (as observed on a screen) is very blurred. This is probably due to scattering of the laser light at surface imperfections of the film. At some of the investigated sample spots, the structural imperfections of the film result in unidirectional laser emission. Examples are shown in Figure 10. At all examined sample spots of the elastomer showing laser emission, we always find a broad contribution to the emission spectrum due to ordinary fluorescence (Figure 10). This is not the case for well-ordered low-molar-mass or highly cross-linked CLC films, where, above the lasing threshold, the laser line dominates the emission.[11]

For constant pump energies, we found a slow variation of the emission intensity and sometimes an abrupt breakdown of laser emission. Waiting several hours

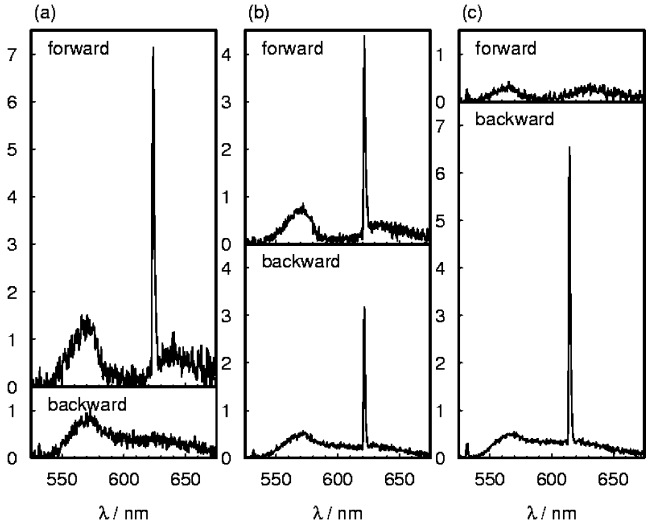


**Figure 10.** Laser emission at different sample spots: unidirectional (a,c) and bidirectional (b) emission (simultaneous detection in the 'forward' and 'backward' direction, as indicated in Figure 1).

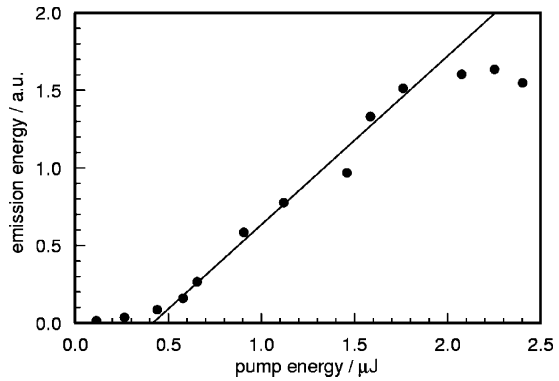


**Figure 11.** Biaxially stretched film: laser emission as a function of pump energy (relative compression of the cholesteric pitch, $p/p_0 = 0.910$; emission wavelength, $\lambda = 604.8$ nm).

after changing the sample deformation in general resulted in improved stability and efficiency of the laser emission. Obviously, strain-induced distortions of the cholesteric order slowly relax during the equilibration of the deformed elastomer film. Due to the limited emission stability, it is difficult to determine lasing thresholds precisely. An example is given in Figure 11, where the laser intensity is plotted as a function of pump energy. The lasing threshold ($W \approx 0.6$ $\mu$J) is not much higher than lasing thresholds of low-molar-mass ($W \approx 0.3$ $\mu$J) or highly cross-linked ($W \approx 0.1$ $\mu$J) films determined under similar experimental conditions.[11]

In Figure 12, the observed laser emission wavelengths for all applied sample deformations are shown as a function of the stop band center wavelength, $\lambda_R$. For a given deformation, the observed lasing wavelength typically varies within a range of about 10 nm, depending on the probed sample spot. In the figure, the region of the stop band is indicated by dashed lines. As found for conventional CLCs doped with DCM, the laser lines are located near the long-wavelength edge of the stop band. One should note that most emission wavelengths seem to be located inside the stop band, in contrast to theory (in CLC films with finite thickness, the resonant modes are not located exactly at the band edges but at a little distance outside the stop band[6]). This discrepancy is probably due to small errors in the determination of the stop band center wavelength, $\lambda_R$, or the refractive indices of the sample (which are needed for the calculation of the band edges). For all applied strains, we never observed laser emission at the short-wavelength band edge—even in the case of the undeformed film, where the optical gain at the short-wavelength band edge is much higher than at the long-wavelength band edge. This can be explained by the positive nematic order parameter of the excited dye's transition dipole moment:[6] the resonant modes at the two band edges resemble continuously twisted, linearly polarized standing waves. The polarization of the resonant mode at the long-wavelength edge is everywhere parallel to the local director, and at the short-wavelength edge, it is everywhere perpendicular to the local director. A preferred orientation of the dye's transition dipole moment parallel to the local director therefore strongly supports lasing at the long-wavelength band edge.

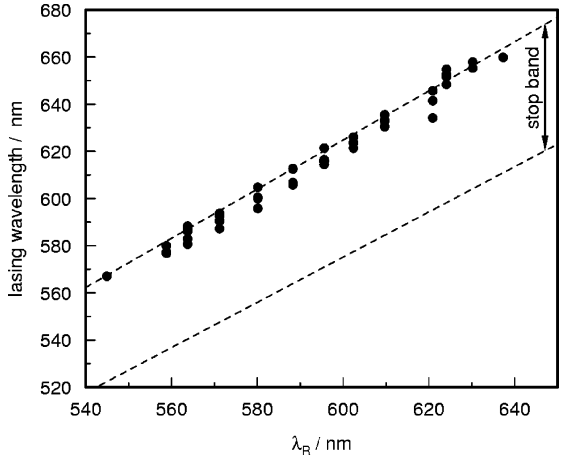


**Figure 12.** Observed laser emission wavelengths as a function of the stop band center, $\lambda_R$. The dashed lines indicate the region of the photonic stop band.

## 4. Conclusions

In this paper, we have presented an optical characterization of a cholesteric elastomer which has been obtained by a new synthetic route, namely by photo-cross-linking a planar-oriented CLC polymer film. Although the chemical constitution is quite similar to films obtained by the anisotropic deswelling method, we find a substantial improvement in the optical properties. The selective reflection band and the photonic effects on emission of fluorescent guest molecules are almost as clear-cut as those found for conventional CLC systems. The cholesteric order is well preserved under biaxial strain, which allows for mechanically tunable band edge laser emission over a wide wavelength range.

In contrast to the strong effect of the cholesteric order on the transmission spectra, its effect on the fluorescence of dispersed dye molecules is surprisingly weak, and the anomalous symmetric emission enhancement at both band edges is not yet understood.

The chosen combination of odd- and even-numbered alkyl spacers of the cholesteric polymer results in a reduced anisotropy of the coil conformation, which seems to be crucial for the formation of a well-ordered cholesteric phase, already in the un-cross-linked sample. This is one possible reason for the limited optical quality of CLC elastomer films formed by the anisotropic deswelling method: This method requires a (locally)

prolate chain conformation to ensure an overall reorientation of the nematic director into the film plane during the deswelling process.

**Acknowledgment.** Thanks are due to the Fonds der Chemischen Industrie and the Deutsche Forschungsgemeinschaft (SFB 428) for financial support.

## References and Notes

(1) de Gennes, P. G.; Prost, J. *The Physics of Liquid Crystals*, 2nd ed.; Clarendon Press: Oxford, 1993.
(2) de Vries, H. *Acta Crystallogr.* **1951**, *4*, 219.
(3) Chen, S. H.; Katsis, D.; Schmid, A. W.; Mastrangelo, J. C.; Tsutsui, T.; Blanton T. N. *Nature* **1999**, *397*, 506.
(4) Kopp, V. I.; Fan, B.; Vithana, H. K. M.; Genack A. Z. *Opt. Lett.* **1998**, *23*, 1707.
(5) Voigt, M.; Chambers, M.; Grell M. *Chem. Phys. Lett.* **2001**, *347*, 173.
(6) Schmidtke J.; Stille W. *Eur. Phys. J. B* **2003**, *31*, 179.
(7) Il'chishin, I. P.; Tikhonov, E. A.; Tishchenko, V. G.; Shpak M. T. *JETP Lett.* **1980**, *32*, 24.
(8) Il'chishin, I. P.; Vakhin, A. Y. *Mol. Cryst. Liq. Cryst.* **1995**, *265*, 687.
(9) Taheri, B.; Muñoz, A. F.; Palffy-Muhoray, P.; Twieg, R. *Mol. Cryst. Liq. Cryst.* **2001**, *358*, 73.
(10) Finkelmann, H.; Kim, S. T.; Muñoz, A.; Palffy-Muhoray, P.; Taheri, B. *Adv. Mater.* **2001**, *13*, 1069.
(11) Schmidtke, J.; Stille, W.; Finkelmann, H.; Kim, S. T. *Adv. Mater.* **2002**, *14*, 746.
(12) Warner, M.; Terentjev, E. M. *Liquid Crystal Elastomers*; Clarendon Press: Oxford, 2003.
(13) Mao, Y.; Terentjev, E. M.; Warner M. *Phys. Rev. E* **2001**, *64*, 041803.
(14) Bermel P. A.; Warner M. *Phys. Rev. E* **2002**, *65*, 056614.
(15) Cicuta, P.; Tajbakhsh, A. R.; Terentjev E. M. *Phys. Rev. E* **2002**, *65*, 051704.
(16) Kim S. T.; Finkelmann H. *Macromol. Rapid Commun.* **2001**, *22*, 429.
(17) Brehmer, M.; Zentel, R.; Wagenblast, G.; Siemensmeyer, K. *Macromol. Chem. Phys.* **1994**, *195*, 1891.
(18) Prucker, O.; Naumann, C. A.; Rühe, J.; Knoll, W.; Frank, C. W. *J. Am. Chem. Soc.* **1999**, *121*, 8766.
(19) Wöhler, H.; Haas, G.; Fritsch, M.; Mlynski, D. A. *J. Opt. Soc. Am. A* **1988**, *5*, 1554.
(20) Berreman, D. W. *J. Opt. Soc. Am.* **1972**, *62*, 502.
(21) Broer, D. J.; Lub, J.; Mol, G. N. *Nature* **1995**, *378*, 467.
(22) Kopp V. I.; Genack A. Z. *Phys. Rev. Lett.* **2001**, *86*, 1753.

MA0487655